

広島大学学術情報リポジトリ

Hiroshima University Institutional Repository

Title	Self-healing polyurethane elastomers based on charge-transfer interactions for biomedical applications
Author(s)	Imato, Keiichi; Nakajima, Hidekazu; Yamanaka, Ryota; Takeda, Naoya
Citation	Polymer Journal , 53 : 355 - 362
Issue Date	2020-09-24
DOI	10.1038/s41428-020-00432-4
Self DOI	
URL	https://ir.lib.hiroshima-u.ac.jp/00051511
Right	This is not the published version. Please cite only the published version. この論文は出版社版ではありません。引用の際には出版社版をご確認、ご利用ください。
Relation	



Self-healing polyurethane elastomers based on charge-transfer interactions for biomedical applications

Running Head: Self-healing elastomers for biomedical applications

Keiichi Imato^{1,2}, Hidekazu Nakajima¹, Ryota Yamanaka¹ and Naoya Takeda¹

¹Department of Life Science and Medical Bioscience, Waseda University (TWIns), 2-2 Wakamatsucho, Shinjuku, Tokyo 162-8480, Japan.

²Department of Applied Chemistry, Hiroshima University, 1-4-1 Kagamiyama, Higashi-Hiroshima 739-8527, Japan.

Correspondence: Dr K Imato, Department of Applied Chemistry, Hiroshima University, 1-4-1 Kagamiyama, Higashi-Hiroshima 739-8527, Japan.

E-mail: kimato@hiroshima-u.ac.jp

or Professor N. Takeda, Department of Life Science and Medical Bioscience, Waseda University (TWIns), 2-2 Wakamatsucho, Shinjuku, Tokyo 162-8480, Japan.

E-mail: ntakeda@waseda.jp

ABSTRACT

One promising application of self-healing polymeric materials is biomedical use. Although charge-transfer (CT) interactions have been employed to construct self-healing polymers as well as other reversible bonds and interactions, their potential for biomedical applications have never been investigated. In this study, we fabricated self-healable and cell-compatible polyurethane elastomers cross-linked by CT complexes between electron-rich pyrene (Py) and electron-deficient naphthalene diimide (NDI) by simple blending of two linear polymers with Py or NDI as a repeating unit. The elastomers at different blend ratios self-healed damage during 1 day in mild conditions including in air

and water at 30–100 °C. The mechanical properties of damaged elastomers were almost restored after healing in air at 100 °C, and even in air at 30 °C and in water at 70 °C, healing was also possible to a certain extent. The good cell-compatibility of the polyurethane elastomers was demonstrated by culturing two kinds of cells on the thin film substrates.

Keywords: biomaterial/cell culture scaffold/charge-transfer interaction/elastomer/self-healing/supramolecular chemistry

INTRODUCTION

Self-healing polymeric materials can repair damage at the macroscopic and molecular levels by the materials themselves in appropriate conditions, which is enabled mainly by reversible bonds/interactions, *i.e.*, dynamic covalent bonds and supramolecular interactions,^{1–7} except for encapsulation and circulation-based engineering systems.^{8,9} The reversible bonds/interactions incorporated in the polymer networks can be cleaved by mechanical stress (damage) in preference to other strong covalent bonds and recombined by external stimuli suitable for each bond/interaction including heating, light irradiation, and pH change. Self-healing is useful particularly in space development¹⁰ and biomedical applications such as artificial tissues and organs,^{11–13} where there is little scope for intervention of repair or replacement and long-term reliability is necessary. Previous self-healing polymeric materials are largely classified into two categories, gels and elastomers, with the single exception of the hard polymer glass.¹⁴ Most studies on self-healing polymers for biomedical applications, however, have focused on hydrogels to use them as 3D cell culture scaffolds in tissue engineering.^{11–13} Although elastomers are available as structural components of artificial tissues and organs and also coatings on them, in which hydrogels cannot be substitutes, to date, self-healable and biocompatible elastomers have rarely reported.^{15–24}

Here we report self-healable and cell-compatible polyurethane elastomers based on the charge-transfer (CT) interaction between electron-rich pyrene (Py) and electron-deficient naphthalene diimide (NDI) as a reversible interaction (Figure 1).²⁵ Unlike hydrogen bonding, one of the most common reversible bonds/interactions in self-healing polymers,^{26,27} CT interactions are hardly affected by water molecules and promise to work in physiological conditions. However, previous self-healing

polymers based on CT interactions have never been investigated for biomedical applications.²⁸⁻³⁴ The reason why we focused on polyurethane is because it has been used in many self-healing polymers³⁵⁻³⁹ and biomaterials with excellent mechanical properties and good biocompatibility.^{40,41} In this paper, we fabricate elastomers with physical cross-links of CT complexes by simply blending two linear polyurethanes containing either Py or NDI as a repeating unit, and evaluate the healing efficiency in various conditions from their mechanical properties. Cell culture on the elastomer surfaces is also performed to demonstrate cell-compatibility.

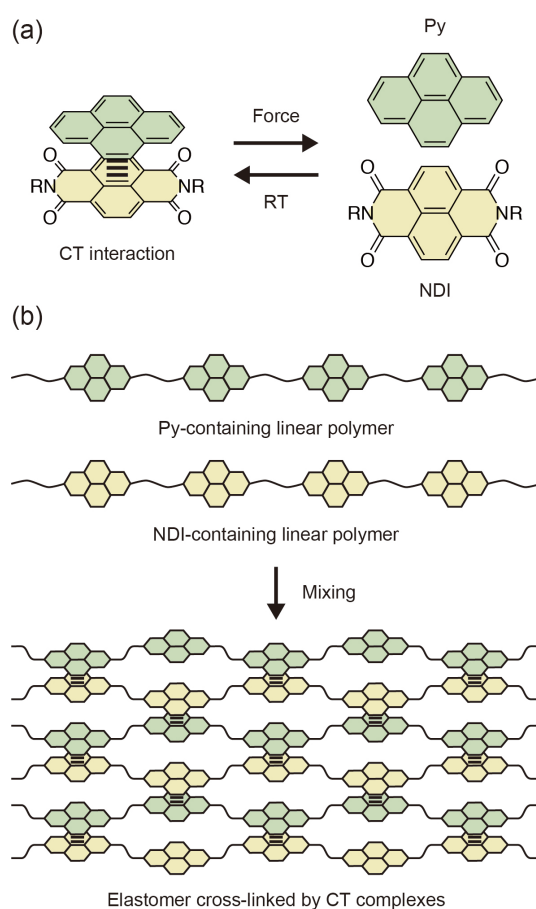


Figure 1 (a) CT interaction between Py and NDI. (b) Facile fabrication of self-healable elastomers with physical cross-links of CT complexes by simple blending of two linear polymers containing Py or NDI as a repeating unit.

EXPERIMENTAL PROCEDURE

Materials

All solvents and reagents were used as received. **Py-diol** and **NDI-diol**, which have two primary hydroxyl groups at both ends, were synthesized according to our previous paper.²⁵ Milli-Q water (resistivity > 18 M Ω cm⁻¹) was prepared using a Milli-Q integral water purification system (ZRXQ003JP, Merck Millipore).

Measurements

¹H NMR spectroscopic measurements were performed at 25 °C in CDCl₃ with tetramethylsilane as the internal standard using a 400-MHz Varian spectrometer. Number-average molecular weights (M_n s) and polydispersity indices (PDIs) of polymers were determined by size exclusion chromatography (SEC) measurements at 40 °C using a JASCO SEC system with a guard column (KF-G 4A, Shodex), two series-connected columns (KF-806L, Shodex), a UV detector, and a differential refractive index detector. Tetrahydrofuran (THF) was used as the eluent, and polystyrene standards were used to calibrate the SEC system. Fluorescence spectra (λ_{ex} = 340 nm) were obtained using a SHIMADZU RF-5300PC spectrofluorometer. UV light (365 nm, UVGL-58, UVP) were used to visualize fluorescence intensity changes. Differential scanning calorimetric (DSC) measurements were performed under N₂ at a heating rate of 10 °C min⁻¹ using a SHIMADZU DSC-60A Plus. Tensile tests were carried out at a strain rate of 30 mm min⁻¹ using rectangular strip specimens (20–30 mm \times ca. 3 mm \times 0.3–0.6 mm) and a SHIMADZU EZ-S instrument equipped with a 5 N load cell. Static water contact angles were measured at three different positions in a substrate by the sessile drop technique using a drop shape analyzer (DSA100S, Krüss).

Polymer synthesis

Two polyurethanes, **Py-PU** and **NDI-PU**, were synthesized by polyaddition of **Py-diol** or **NDI-diol**, poly(tetramethylene glycol) (PTMG, M_n = 2 000), and 4,4'-diphenylmethane diisocyanate (MDI) in the presence of a tin catalyst, di-*n*-butyltin dilaurate (DBTDL).

Py-PU. A solution of **Py-diol** (260 mg, 0.742 mmol), PTMG (2.97 g, 1.49 mmol), and MDI (558 mg, 2.23 mmol) in anhydrous *N,N*-dimethylformamide (DMF, 16 mL) was prepared under N₂ atmosphere. A THF solution of 10 vol% DBTDL (1 drop) was added into the mixture, and the mixture

was stirred at 70 °C. After 24 h, the mixture was cooled to room temperature and precipitated in MeOH. The precipitate was collected and dried *in vacuo* at room temperature to give **Py-PU** (3.03 g, 80% yield). ¹H NMR (400 MHz, CDCl₃): δ (ppm) = 7.93 (m, 4H, Py aromatic), 7.69 (m, 4H, Py aromatic), 7.29 (m, 4H, MDI aromatic), 7.09 (d, *J* = 8.0 Hz, 4H, MDI aromatic), 6.71 (br, NH), 4.47 (t, *J* = 6.6 Hz, 4H, Py CH₂), 4.37 (t, *J* = 6.4 Hz, 4H, Py CH₂), 3.88 (s, 2H, MDI CH₂), 3.41 (m, 4H, PTMG CH₂), 2.30 (m, 4H, Py CH₂), 1.62 (m, 4H, PTMG CH₂) (Supplementary Figure S1). *M_n* = 38 900 g mol⁻¹, PDI = 2.00.

NDI-PU. A solution of **NDI-diol** (475 mg, 1.07 mmol), PTMG (4.30 g, 2.15 mmol), and MDI (807 mg, 3.22 mmol) in anhydrous DMF (23.6 mL) was prepared under N₂ atmosphere. A THF solution of 10 vol% DBTDL (1 drop) was added into the mixture, and the mixture was stirred at 70 °C. After 24 h, the mixture was cooled to room temperature and precipitated in MeOH. The precipitate was collected and dried *in vacuo* at room temperature to give **NDI-PU** (4.65 g, 83% yield). ¹H NMR (400 MHz, CDCl₃): δ (ppm) = 8.61 (m, 4H, NDI aromatic), 7.29 (m, 4H, MDI aromatic), 7.09 (d, *J* = 8.4 Hz, 4H, MDI aromatic), 6.78 (br, NH), 4.46 (m, 4H, NDI CH₂), 4.23 (m, 4H, NDI CH₂), 3.88 (m, 4H, NDI CH₂ and 2H, MDI CH₂), 3.76 (m, 4H, NDI CH₂), 3.41 (m, 4H, PTMG CH₂), 1.62 (m, 4H, PTMG CH₂) (Supplementary Figure S2). *M_n* = 39 000 g mol⁻¹, PDI = 1.98.

Elastomer preparation

Blend samples of **Py-PU** and **NDI-PU** at the different ratios of **Py-PU/NDI-PU** (wt/wt) = 1/0, 2/1, 1/1, 1/2, and 0/1 were prepared. Each polymer mixture (960 mg in total) was dissolved in CHCl₃ (12 mL), filtered, cast on a Teflon dish, and dried at room temperature in air overnight and *in vacuo* for 2 h to obtain a thick film (0.3–0.6 mm thickness).

Healing efficiency

Healing efficiency of the blend thick films was evaluated from the recovery of elongation at break and maximum stress in tensile tests. A 1 mm nick was made at the center of a rectangular strip specimen (20–30 mm × ca. 3 mm × 0.3–0.6 mm) with a razor blade, and the freshly cut surfaces were immediately made contacted with each other and pressed firmly. After healing in air or water at different temperatures (30–100 °C) for different time periods (0–24 h), tensile tests were performed using more than three

specimens for each healing condition; three of them were chosen for the average values of the elongation at break and maximum stress.

Cell-compatibility

Cell-compatibility of the blend elastomer at **Py-PU/NDI-PU** (wt/wt) = 1/1 was evaluated from cell culture on its thin films. The **Py-PU/NDI-PU** mixture (20 mg) was dissolved in CHCl_3 (4 mL), and 360 μL of the solution was used to spin-coat it on a cover glass (24 mm \times 24 mm, 0.13–0.25 mm thickness, Matsunami Glass) without any surface pretreatment at 3 000 rpm for 30 s using a spin coater (ACT-300D, Active). The elastomer-coated glasses were dried in air at room temperature for 1 day. Prior to cell seeding, the substrates were exposed to UV light for 15 min at room temperature for sterilization. Bovine aortic endothelial cells (BAECs, P8, Cell Applications) and mouse myoblast (C2C12) cells (P9, RIKEN Cell Bank) were seeded on the elastomer-coated substrates (10% confluent) and cultured at 37 °C with 5% CO_2 in Dulbecco's modified Eagle's medium with high glucose containing 10% fetal bovine serum and 1% penicillin and streptomycin. Cell culture on the tissue culture polystyrene (TCPS) dishes was also conducted as a control experiment. The number of adhered cells was calculated by counting the cells collected upon trypsin-ethylenediaminetetraacetic acid treatment. Cell imaging was carried out using a Nikon Eclipse Ti-E/B phase contrast microscope. For fluorescent imaging, BAECs cultured on the elastomer-coated substrate for 3 days were fixed with 4% paraformaldehyde, and the nuclei and F-actin were fluorescently stained with Hoechst 33342 and Alexa Fluor 568 Phalloidin, respectively. The stained cells were observed using a Nikon Eclipse TE2000-U inverted microscope.

RESULTS AND DISCUSSION

Polymer synthesis

Two polyurethanes containing either Py or NDI as a repeating unit, **Py-PU** and **NDI-PU**, were synthesized by polyaddition of dihydroxyl Py (**Py-diol**) or NDI (**NDI-diol**), dihydroxyl-terminated PTMG ($M_n = 2\ 000$), and small diisocyanate (MDI) in the presence of a tin catalyst (DBTDL), as shown in Figure 2.^{42–44} Both polyurethanes have large M_n s enough for mechanical evaluation and remarkably similar M_n s, PDIs, and compositions (Table 1). Compared with the feed ratios, smaller amounts of Py

and NDI were incorporated into the polymers (Supplementary Figure S1 and S2).

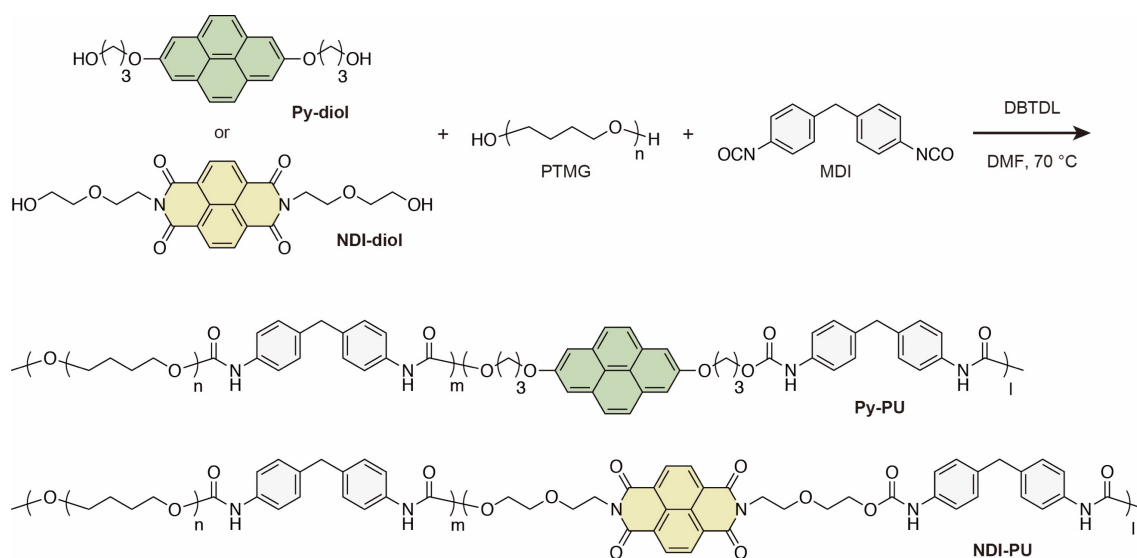


Figure 2 Synthetic scheme for **Py-PU** and **NDI-PU** by polyaddition.

Table 1 M_{ns} , PDIs, and compositions of **Py-PU** and **NDI-PU**

	Molar ratio ^a (Feed ratio)			M_n^b	PDI ^b
	Py or NDI	PTMG	MDI		
Py-PU	1 (1)	3.4 (2)	4.4 (3)	38 900	2.00
NDI-PU	1 (1)	2.6 (2)	3.6 (3)	39 000	1.98

^aCalculated from ¹H NMR. ^bDetermined from SEC.

Preparation and characterization of elastomers

The cast thick films of **Py-PU** and **NDI-PU** showed brown and orange color, respectively (Figure 3a). Blending the polyurethanes produced dark red films, the color of which indicates the formation of CT complexes between Py and NDI units.^{25,29,31,34} The CT complexation was also confirmed from their fluorescence spectra in a CHCl₃ solution (Figure 3b).^{25,29,31} The intense fluorescence from Py was drastically attenuated in the 1/1 blend solution by the CT complexation. The fluorescence quenching was clearly observed in the solution by the naked eye under UV light irradiation.

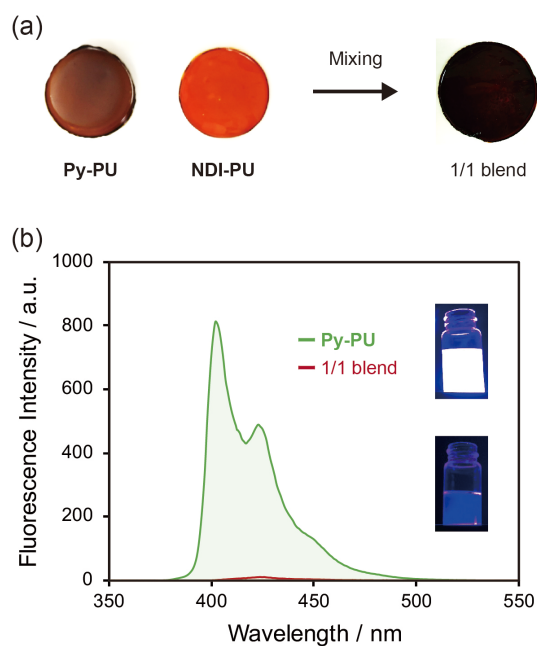


Figure 3 (a) Photographs of cast thick films of **Py-PU**, **NDI-PU**, and **Py-PU/NDI-PU** (wt/wt) = 1/1 blend. (b) Fluorescence spectra ($\lambda_{\text{ex}} = 340 \text{ nm}$) of **Py-PU** (5 mg mL^{-1}) and the **Py-PU/NDI-PU** (wt/wt) = 1/1 blend (10 mg mL^{-1}) in CHCl_3 . Inserts are photographs of the **Py-PU** (top) and 1/1 blend (bottom) solutions under UV light (365 nm).

The DSC curve showed that the 1/1 blend has two glass transition temperatures (T_{gs}) and one melting temperature (T_{m}), which are similarly observed in **Py-PU** and **NDI-PU** (Figure 4a). The two T_{gs} and transparency of the films indicate that the materials are phase-separated at the micro level. The glass transition around $-70 \text{ }^\circ\text{C}$ and melting around $15 \text{ }^\circ\text{C}$ originate from the crystalline PTMG.⁴⁵ The glass transition around $90 \text{ }^\circ\text{C}$ is attributed to the hard domains mainly composed of the hard segments with high densities of the urethane linkages, which consist of Py, NDI, and MDI and can statistically generate in the polymerization. As a consequence, the two polyurethanes and their blends are non-crystalline and amorphous elastomers with physical cross-links in the glassy domains: CT complexes between Py and NDI and hydrogen bonding between the urethane linkages at room temperature.

Py-PU resisted high strain and stress to show a good mechanical property in the tensile tests, whereas **NDI-PU** is extremely weak (Figure 4b). The difference is probably due to the microstructures of but unrecognizable in the DSC curves. Blending the polyurethanes resulted in tough elastomers with excellent mechanical properties. This would be caused by the formation of CT complexes as physical

cross-links, which can effectively dissipate energy by the dissociation upon mechanical stress.^{46,47}

Particularly, the blends at the ratios of **Py-PU/NDI-PU** (wt/wt) = 2/1 and 1/1 showed the highest maximum stress and elongation at break, respectively, in the tensile tests.

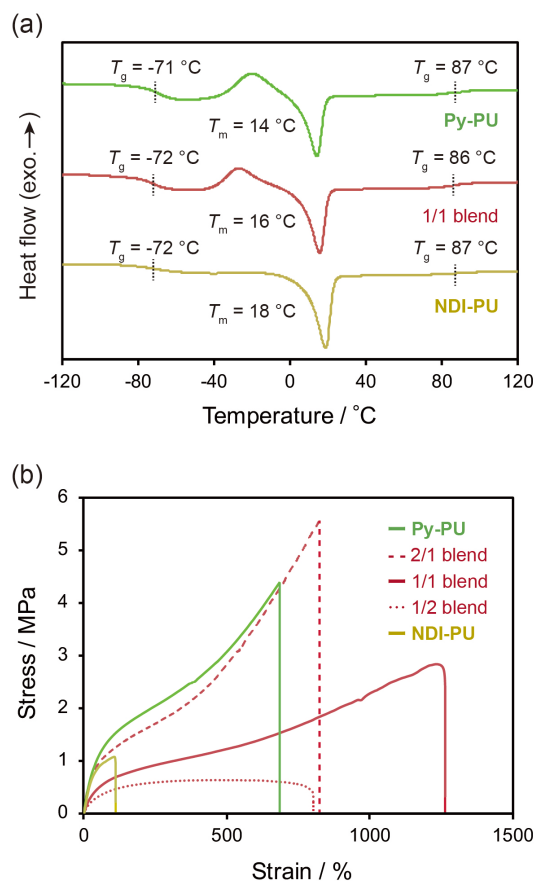


Figure 4 (a) DSC curves of **Py-PU** (green, top), **NDI-PU** (yellow, bottom), and their 1/1 blend (red, center). (b) Typical stress-strain curves of cast thick films of **Py-PU** (green), **NDI-PU** (yellow), and their 2/1 (red dashed line), 1/1 (red solid line), and 1/2 blends (red dotted line).

Self-healing

We mainly focused on the 1/1 blend with the excellent mechanical property (elongation at break) and investigated its self-healing behavior (Supplementary Figure S3 and S4). As the experiment procedure is shown in Figure 5a, a 1 mm nick was made at the center of a rectangular strip film, the freshly cut surfaces were immediately made contacted with each other and strongly pressed, and the film was placed in each condition to undergo healing, whose medium (air or water), temperature (30–100 °C), and time

period (0–24 h) were varied. After healing, the specimens were stretched to measure the mechanical properties. The stress-strain curves of the damaged specimens gradually recovered to the intact one with increasing the temperature in the healing in air for 24 h (Figure 5b). The specimens after healing at 30 and 70 °C fractured at the nick in the tensile tests, whereas those after healing at 100 °C broke at random positions similar to the intact ones, which indicates that the mechanical properties were almost restored. The healing efficiency was determined from the recovery of elongation at break and maximum stress in the curves (Figure 5c). The healing in air at 30, 70, and 100 °C for 24 h enabled the recovery of nearly 40%, 60%, and 80%, respectively. Even in the mild condition at 30 °C close to body temperature, healing was possible to a certain extent. During the healing processes at all temperatures including 100 °C, the specimens were not fluid but retained the original shapes at the macroscopic level, although the DSC curves suggest the liquefaction of the blends around 90 °C. This would indicate that the physical cross-links such as CT complexes between Py and NDI and hydrogen bonding between the urethane linkages⁴⁵ maintained the polymer network structures. Therefore, we concluded that the blend elastomers healed damage by themselves without melting.

The increase in the time period was also effective for a better healing (Supplementary Figure S5). In addition, such healing was observed in the other blends at the **Py-PU/NDI-PU** (wt/wt) = 2/1 and 1/2 ratios (Supplementary Figure S6). To explore the potential of use in physiological conditions, healing in water was investigated (Supplementary Figure S7). Although the efficiency was lower than that in air, healing was possible to a certain extent in water. The reason for the lower efficiency is probably because water penetrated into the nick and physically interfered with the healing.

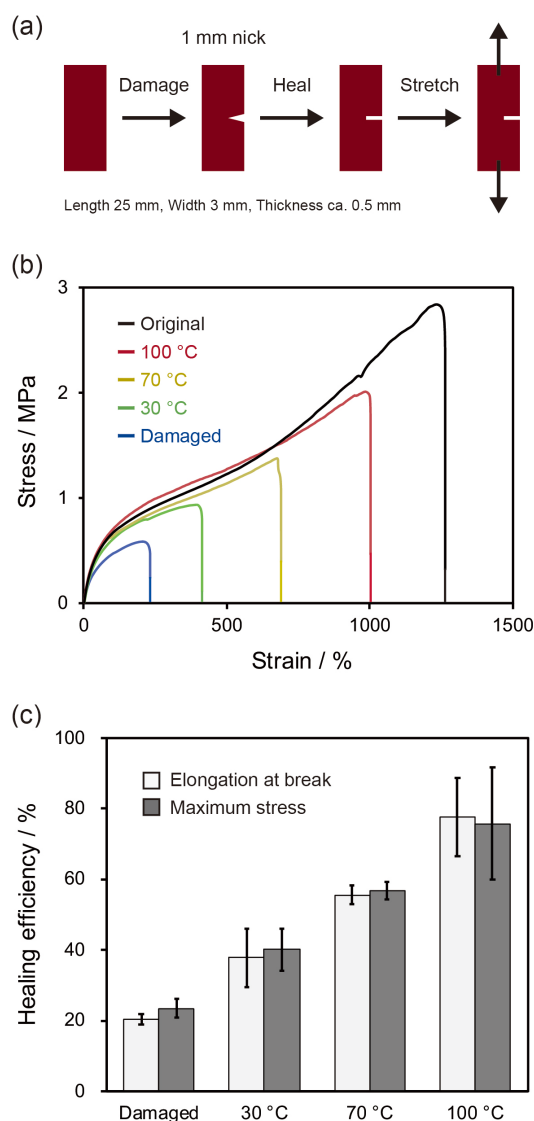


Figure 5 (a) Illustration of quantitative evaluation of healing efficiency by tensile tests. (b and c) Temperature effect on healing behavior of the 1/1 blend elastomer film. (b) Typical stress-strain curves of the thick films without (black) and with a nick (blue) and after healing in air at 30 (green), 70 (yellow), and 100 °C (red) for 24 h. (c) Healing efficiency estimated from elongation at break (white) and maximum stress (gray) in the tensile tests (Mean \pm SD, $n = 3$).

Cell-compatibility

For biomedical use of the self-healable blend elastomers, the cell-compatibility was evaluated by culturing two kinds of cells, C2C12 cells and BAECs, on the elastomer surfaces. C2C12 cells were selected because of matching as the precursor cells of self-healable muscle tissue and strong adhesion property, while BAECs were employed to examine the behaviors of weak adhesion cells. Thin films of

the 1/1 blend elastomer were fabricated on glass substrates by spin-coating (thickness < 100 nm),⁴⁸ and the cells were seeded on the surfaces. Both cells adhered to the substrates, extended, and proliferated well (Figure 6). One possible reason for the strong adhesion is the hydrophobicity of the surfaces, which showed a water contact angle of $80.2^\circ \pm 3.8^\circ$. It is well known that most adhesive cells and cell-adhesive proteins prefer hydrophobic surfaces with water contact angles around $70\text{--}80^\circ$.⁴⁹ The nuclei and F-actin were fluorescently stained in BAECs cultured on the substrate for 3 days to investigate the cell adhesion in detail (Figure 7). The fluorescence microscopic image showed that the BAECs remarkably formed actin stress fibers to indicate strong adhesion on the surface with metabolic activity. Furthermore, the doubling time of BAECs was 16.7 h, which was comparable to that on TCPS (15.8 h). From these results, we concluded that the blend elastomers have good cell-compatibility as expected.

Interestingly, C2C12 cells did not adhere to the cast thick film of the 1/1 blend (thickness = 0.3–0.6 mm, Supplementary Figure S8). Because moduli of culture scaffolds strongly affect cell adhesion,⁵⁰ the thick film without a stiff glass substrate would be soft for C2C12 cells. This result potentially suggests that if the blend elastomers are employed as coatings on artificial tissues and organs, we can select whether the surfaces are cell-adhesive or not for the intended use by the thickness.

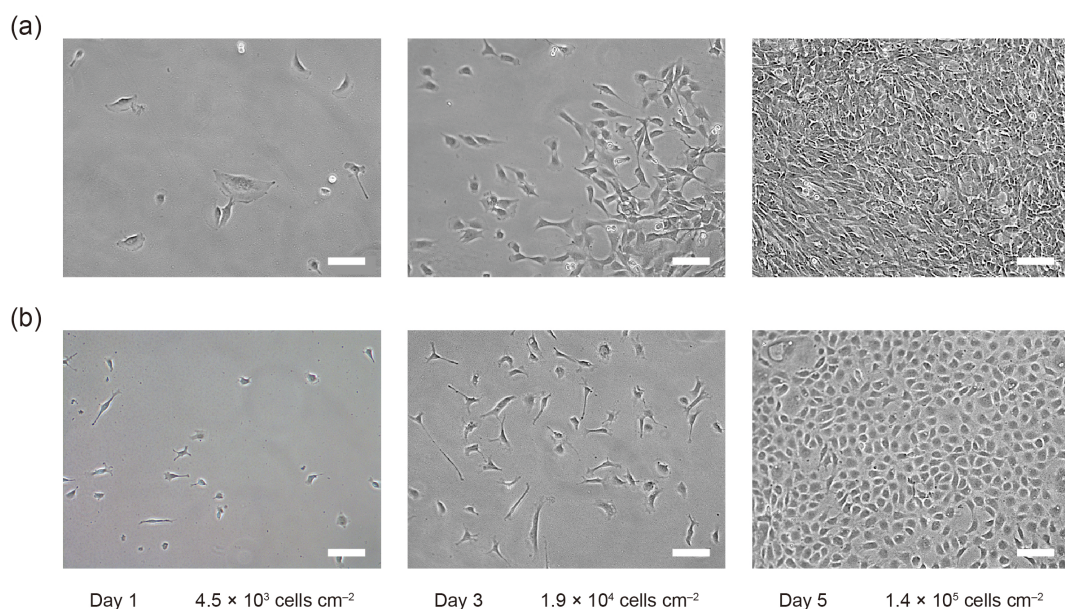


Figure 6 Phase-contrast microscopic images of (a) C2C12 cells and (b) BAECs cultured on the 1/1 blend thin films for 1, 3, or 5 day(s). Scale bars are 100 μm .

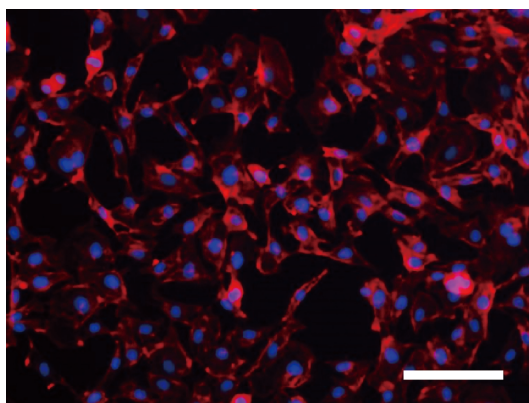


Figure 7 Microscopic image of fluorescent-stained BAECs nuclei (blue) and F-actin (red) on the 1/1 blend thin film at 3 days culture. Scale bar is 100 μm .

CONCLUSION

In this study, we fabricated the self-healable and cell-compatible elastomers cross-linked by the reversible CT complexes between electron-rich Py and electron-deficient NDI units by simply blending the two linear polyurethanes with either Py or NDI as a repeating unit but remarkably similar chemical structures (M_n s, PDIs, and compositions). The blend elastomers at different Py/NDI ratios healed damage by themselves during 1 day in mild conditions such as in air and water at 30–100 °C. The healing efficiency was quantitatively evaluated from the recovery of mechanical properties measured by tensile tests. Nearly 80% recovery was possible without liquefaction after healing in air at 100 °C, while healing to a certain extent was also observed in air at 30 °C and in water at 70 °C. The good proliferation of C2C12 cells and BAECs on their thin film substrates demonstrated the cell-compatibility of the elastomers. This study investigated the potential of self-healable elastomers based on CT interactions for biomedical use for the first time in spite of their recent intense researches. We believe that the findings obtained in this study will contribute to the development of self-healable polymeric biomaterials based on reversible bonds/interactions.

CONFLICT OF INTEREST

The authors declare no conflict of interest.

ACKNOWLEDGEMENTS

This work was supported by JSPS KAKENHI (Grant No. 16H07292 and 19K15623, K.I.), MEXT LEADER (Grant No. A6501, K.I.), and Izumi Science and Technology Foundation (Grant No. H29-J-113, K.I.). A research grant of Mitsubishi Materials–Faculty of Science and Engineering, Waseda University (2016, 2018) and Grant for Young Scientists Encouragement of Waseda Research Institute for Science and Engineering–JXTG Energy (2017) are also acknowledged for financial support.

REFERENCES

1. Herbst, F., Döhler, D., Michael, P. & Binder, W. H. Self-healing polymers via supramolecular forces. *Macromol. Rapid Commun.* **34**, 203–220 (2013).
2. Harada, A., Takashima, Y. & Nakahata, M. Supramolecular polymeric materials via cyclodextrin–guest interactions. *Acc. Chem. Res.* **47**, 2128–2140 (2014).
3. Roy, N., Bruchmann, B. & Lehn, J.-M. DYNAMERS: dynamic polymers as self-healing materials. *Chem. Soc. Rev.* **44**, 3786–3807 (2015).
4. Yang, Y., Ding, X. & Urban, M. W. Chemical and physical aspects of self-healing materials. *Prog. Polym. Sci.* **49-50**, 34–59 (2015).
5. Imato, K. & Otsuka, H. in *Dynamic Covalent Chemistry: Principles, Reactions and Applications* (eds Zhang, W. & Jin, Y.) 359–387 (John Wiley & Sons, Hoboken, NJ, USA, 2017).
6. Imato, K. & Otsuka, H. Reorganizable and stimuli-responsive polymers based on dynamic carbon-carbon linkages in diarylbibenzofuranones. *Polymer* **137**, 395–413 (2018).
7. Dahlke, J., Zechel, S., Hager, M. D. & Schubert, U. S. How to design a self-healing polymer: general concepts of dynamic covalent bonds and their application for intrinsic healable materials. *Adv. Mater. Interfaces* **50**, 1800051 (2018).
8. Diesendruck, C. E., Sottos, N. R., Moore, J. S. & White, S. R. Biomimetic self-healing. *Angew. Chem. Int. Ed.* **54**, 10428–10447 (2015).
9. Patrick, J. F., Robb, M. J., Sottos, N. R., Moore, J. S. & White, S. R. Polymers with autonomous life-cycle control. *Nature* **540**, 363–370 (2016).

10. Levchenko, I., Bazaka, K., Belmonte, T., Keidar, M. & Xu, S. Advanced materials for next-generation spacecraft. *Adv. Mater.* **41**, 1802201 (2018).
11. Tu, Y., Chen, N., Li, C., Liu, H., Zhu, R., Chen, S., Xiao, Q., Liu, J., Ramakrishna, S. & He, L. Advances in injectable self-healing biomedical hydrogels. *Acta Biomater.* **90**, 1–20 (2019).
12. Talebian, S., Mehrali, M., Taebnia, N., Pennisi, C. P., Kadumudi, F. B., Foroughi, J., Hasany, M., Nikkhah, M., Akbari, M., Orive, G. & Dolatshahi-Pirouz, A. Self-healing hydrogels: the next paradigm shift in tissue engineering? *Adv. Sci.* **6**, 1801664 (2019).
13. Uman, S., Dhand, A. & Burdick, J. A. Recent advances in shear-thinning and self-healing hydrogels for biomedical applications. *J. Appl. Polym. Sci.* **336**, 48668–20 (2019).
14. Yanagisawa, Y., Nan, Y., Okuro, K. & Aida, T. Mechanically robust, readily repairable polymers via tailored noncovalent cross-linking. *Science* **359**, 72–76 (2018).
15. Zhao, J., Xu, R., Luo, G., Wu, J. & Xia, H. Self-healing poly(siloxane-urethane) elastomers with remoldability, shape memory and biocompatibility. *Polym. Chem.* **7**, 7278–7286 (2016).
16. Zhao, J., Xu, R., Luo, G., Wu, J. & Xia, H. A self-healing, re-moldable and biocompatible crosslinked polysiloxane elastomer. *J. Mater. Chem. B* **4**, 982–989 (2016).
17. Daemi, H., Rajabi-Zeleti, S., Sardon, H., Barikani, M., Khademhosseini, A. & Baharvand, H. A robust super-tough biodegradable elastomer engineered by supramolecular ionic interactions. *Biomaterials* **84**, 54–63 (2016).
18. Chen, S., Bi, X., Sun, L., Gao, J., Huang, P., Fan, X., You, Z. & Wang, Y. Poly(sebacoyl diglyceride) cross-linked by dynamic hydrogen bonds: a self-healing and functionalizable thermoplastic bioelastomer. *ACS Appl. Mater. Interfaces* **8**, 20591–20599 (2016).
19. Wu, Y., Wang, L., Zhao, X., Hou, Sen, Guo, B. & Ma, P. X. Self-healing supramolecular bioelastomers with shape memory property as a multifunctional platform for biomedical applications via modular assembly. *Biomaterials* **104**, 18–31 (2016).
20. Liu, L., Zhu, L. & Zhang, L. A solvent-resistant and biocompatible self-healing supramolecular elastomer with tunable mechanical properties. *Macromol. Chem. Phys.* **219**, 1700409–7 (2017).
21. Tallia, F., Russo, L., Li, S., Orrin, A. L. H., Shi, X., Chen, S., Steele, J. A. M., Meille, S., Chevalier, J., Lee, P. D., Stevens, M. M., Cipolla, L. & Jones, J. R. Bouncing and 3D printable hybrids with

- self-healing properties. *Mater. Horiz.* **5**, 849–860 (2018).
22. Li, F., Ye, Q., Gao, Q., Chen, H., Shi, S. Q., Zhou, W., Li, X., Xia, C. & Li, J. Facile fabrication of self-healable and antibacterial soy protein-based films with high mechanical strength. *ACS Appl. Mater. Interfaces* **11**, 16107–16116 (2019).
 23. Liu, J., Duan, W., Song, J., Guo, X., Wang, Z., Shi, X., Liang, J., Wang, J., Cheng, P., Chen, Y., Zaworotko, M. J. & Zhang, Z. Self-healing hyper-cross-linked metal–organic polyhedra (HCMOPs) membranes with antimicrobial activity and highly selective separation properties. *J. Am. Chem. Soc.* **141**, 12064–12070 (2019).
 24. Zeimaran, E., Pourshahrestani, S., Kadri, N. A., Kong, D., Shirazi, S. F. S., Naveen, S. V., Murugan, S. S., Kumaravel, T. S. & Salamatina, B. Self-healing polyester urethane supramolecular elastomers reinforced with cellulose nanocrystals for biomedical applications. *Macromol. Biosci.* **19**, 1900176–12 (2019).
 25. Imato, K., Yamanaka, R., Nakajima, H. & Takeda, N. Fluorescent supramolecular mechanophores based on charge-transfer interactions. *Chem. Commun.* **56**, 7937–7940 (2020).
 26. Cordier, P., Tournilhac, F., Soulié-Ziakovic, C. & Leibler, L. Self-healing and thermoreversible rubber from supramolecular assembly. *Nature* **451**, 977–980 (2008).
 27. Tamate, R., Hashimoto, K., Horii, T., Hirasawa, M., Li, X., Shibayama, M. & Watanabe, M. Self-healing micellar ion gels based on multiple hydrogen bonding. *Adv. Mater.* **30**, 1802792–7 (2018).
 28. Burattini, S., Colquhoun, H. M., Fox, J. D., Friedmann, D., Greenland, B. W., Harris, P. J. F., Hayes, W., Mackay, M. E. & Rowan, S. J. A self-repairing, supramolecular polymer system: healability as a consequence of donor–acceptor π – π stacking interactions. *Chem. Commun.* 6717–6719 (2009).
 29. Burattini, S., Greenland, B. W., Merino, D. H., Weng, W., Seppala, J., Colquhoun, H. M., Hayes, W., Mackay, M. E., Hamley, I. W. & Rowan, S. J. A healable supramolecular polymer blend based on aromatic π – π stacking and hydrogen-bonding interactions. *J. Am. Chem. Soc.* **132**, 12051–12058 (2010).
 30. Fox, J., Wie, J. J., Greenland, B. W., Burattini, S., Hayes, W., Colquhoun, H. M., Mackay, M. E. & Rowan, S. J. High-strength, healable, supramolecular polymer nanocomposites. *J. Am. Chem. Soc.* **134**, 5362–5368 (2012).

31. Hart, L. R., Harries, J. L., Greenland, B. W., Colquhoun, H. M. & Hayes, W. Supramolecular approach to new inkjet printing inks. *ACS Appl. Mater. Interfaces* **7**, 8906–8914 (2015).
32. Hart, L. R., Nguyen, N. A., Harries, J. L., Mackay, M. E., Colquhoun, H. M. & Hayes, W. Perylene as an electron-rich moiety in healable, complementary π - π stacked, supramolecular polymer systems. *Polymer* **69**, 293–300 (2015).
33. Qin, J., Lin, F., Hubble, D., Wang, Y., Li, Y., Murphy, I. A., Jang, S.-H., Yang, J. & Jen, A. K. Y. Tuning self-healing properties of stiff, ion-conductive polymers. *J. Mater. Chem. A* **7**, 6773–6783 (2019).
34. Xiao, W.-X., Liu, D., Fan, C.-J., Xiao, Y., Yang, K.-K. & Wang, Y.-Z. A high-strength and healable shape memory supramolecular polymer based on pyrene-naphthalene diimide complexes. *Polymer* **190**, 122228 (2020).
35. Imato, K., Takahara, A. & Otsuka, H. Self-healing of a cross-linked polymer with dynamic covalent linkages at mild temperature and evaluation at macroscopic and molecular levels. *Macromolecules* **48**, 5632–5639 (2015).
36. Imato, K., Natterodt, J. C., Sapkota, J., Goseki, R., Weder, C., Takahara, A. & Otsuka, H. Dynamic covalent diarylbibenzofuranone-modified nanocellulose: mechanochromic behaviour and application in self-healing polymer composites. *Polym. Chem.* **8**, 2115–2122 (2017).
37. Kim, S.-M., Jeon, H., Shin, S.-H., Park, S.-A., Jegal, J., Hwang, S. Y., Oh, D. X. & Park, J. Superior toughness and fast self-healing at room temperature engineered by transparent elastomers. *Adv. Mater.* **30**, 1705145–8 (2018).
38. Zhang, L., Liu, Z., Wu, X., Guan, Q., Chen, S., Sun, L., Guo, Y., Wang, S., Song, J., Jeffries, E. M., He, C., Qing, F. L., Bao, X. & You, Z. A highly efficient self-healing elastomer with unprecedented mechanical properties. *Adv. Mater.* **31**, 1901402–8 (2019).
39. Hornat, C. C. & Urban, M. W. Entropy and interfacial energy driven self-healable polymers. *Nat. Commun.* **11**, 1028 (2020).
40. Gunatillake, P. A., Adhikari, R. & Gadegaard, N. Biodegradable synthetic polymers for tissue engineering. *Eur. Cells Mater.* **5**, 1–16 (2003).
41. Teo, A. J. T., Mishra, A., Park, I., Kim, Y.-J., Park, W. T. & Yoon, Y. J. Polymeric biomaterials for

- medical implants and devices. *ACS Biomater. Sci. Eng.* **2**, 454–472 (2016).
42. Imato, K., Nishihara, M., Kanehara, T., Amamoto, Y., Takahara, A. & Otsuka, H. Self-healing of chemical gels cross-linked by diarylbibenzofuranone-based trigger-free dynamic covalent bonds at room temperature. *Angew. Chem. Int. Ed.* **51**, 1138–1142 (2012).
 43. Imato, K., Ohishi, T., Nishihara, M., Takahara, A. & Otsuka, H. Network reorganization of dynamic covalent polymer gels with exchangeable diarylbibenzofuranone at ambient temperature. *J. Am. Chem. Soc.* **136**, 11839–11845 (2014).
 44. Imato, K., Irie, A., Kosuge, T., Ohishi, T., Nishihara, M., Takahara, A. & Otsuka, H. Mechanophores with a reversible radical system and freezing-induced mechanochemistry in polymer solutions and gels. *Angew. Chem. Int. Ed.* **54**, 6168–6172 (2015).
 45. Imato, K., Kanehara, T., Nojima, S., Ohishi, T., Higaki, Y., Takahara, A. & Otsuka, H. Repeatable mechanochemical activation of dynamic covalent bonds in thermoplastic elastomers. *Chem. Commun.* **52**, 10482–10485 (2016).
 46. Sun, T. L., Kurokawa, T., Kuroda, S., Ihsan, A. B., Akasaki, T., Sato, K., Haque, M. A., Nakajima, T. & Gong, J. P. Physical hydrogels composed of polyampholytes demonstrate high toughness and viscoelasticity. *Nat. Mater.* **12**, 932–937 (2013).
 47. Nakahata, M., Takashima, Y. & Harada, A. Highly flexible, tough, and self-healing supramolecular polymeric materials using host-guest interaction. *Macromol. Rapid Commun.* **37**, 86–92 (2016).
 48. He, D., Arisaka, Y., Masuda, K., Yamamoto, M. & Takeda, N. A photoresponsive soft interface reversibly controls wettability and cell adhesion by conformational changes in a spiropyran-conjugated amphiphilic block copolymer. *Acta Biomater.* **51**, 101–111 (2017).
 49. Tamada, Y. & Yoshito, I. Effect of preadsorbed proteins on cell adhesion to polymer surfaces. *J. Colloid Interface Sci.* **155**, 334–339 (1993).
 50. Li, Y., Xiao, Y. & Liu, C. The Horizon of Materiobiology: A perspective on material-guided cell behaviors and tissue engineering. *Chem. Rev.* **117**, 4376–4421 (2017).

GRAPHICAL ABSTRACT

